International Research Journal of Engineering and Technology (IRJET) e-ISSN: 2395-0056
Volume: 07 Issue: 05 | May 2020 www.irjet.net p-ISSN: 2395-0072

COMPUTATIONAL ANALYSIS OF BLENDED WING BODY UAV CONFIGURATION WITH FLAPS

Suresh P[1], Shreya G[2], Vinutha G[3], Isha G[4], Shreya M[5]

[1]*Asst. Professor, Dept. of Aeronautical Engineering, Dayananda Sagar College of Engineering, Karnataka, India*
[2,3,4,5] *Student, Dept. of Aeronautical Engineering, Dayananda Sagar College of Engineering, Karnataka, India*

Abstract

The requirement to design an eco-friendly aircraft that can produce higher lift which is aerodynamically efficient has directed the designers to develop the Blended Wing Body (BWB) aircraft concept. The benefits of this kind of aircraft mainly arises due to distributed structural and aerodynamic loads, which leads to better aerodynamic performance and provides lighter structural weight as well. In comparison with the conventional wing and fuselage design, BWB design has been proved to have noteworthy enhancements in terms of aerodynamic efficiency. However, it is challenging to design BWB with high lift devices, especially trailing edge devices because of its inability to counteract the significant pitching moments. Due to its large wing area, greater lift to drag ratio, it was observed that high lift devices could be effectively used in BWB aircraft, in terms of longitudinal stability, such that it would meet take-off and landing requirements for a field length comparable to that of conventional aircrafts.

In this present study an attempt has been made to design a Blended Wing Body UAV with and without flaps using Solidworks 2018 and analyzing it through CFD approach using ANSYS 18.1. Also, the improvement in the lift generation and increase in L/D ratio can be verified with the previously designed BWB UAV without flaps model.

Key Words: **Aerodynamically efficient, large wing area, greater lift to drag ratio, high lift devices, longitudinal stability, CFD approach.**

1. INTRODUCTION

1.1.Unmanned Aerial Vehicle (UAV)

An unmanned aerial vehicle can be defined as any type of aerial vehicle without a human pilot on board. UAV's can be of various types including rotor wing aircraft, fixed wing aircraft, etc. Here we refer aerial unmanned vehicles to fixed-wing aerial vehicles. UAV's are controlled by human pilots from a remote distance or can be fully autonomous. In this case, the auto-piloting software is integrated in on-board computers. The flight path for a specific mission can be pre-programmed into the memory of the onboard computer.

1.2. Blended Wing Body (BWB)

Blended Wing Body (BWB) is a concept where fuselage is merged with wing and tail to become a single entity. The major difference of this BWB concept is the way it generates lift. Conventional aircraft obtains its lift from its wings where as BWB aircraft obtains lift from fuselage along with its wings. The control surfaces of the wing are located along the leading and trailing edges of the wing and on the winglets. To conclude, the BWB aircraft configuration, has the ability to provide a great number of benefits through its structural concepts, such as its aerodynamically low interface drag, high lift-to-drag ratio, structurally favorable span loading, and the reduction of greenhouse emissions.

1.3. High lift devices and effect of flaps on the aircraft

In aircraft design and aerospace engineering, a high-lift device is an element or mechanism on an aircraft's wing that augments the amount of lift produced by the wing. The device may be a fixed component, or a movable mechanism which is installed when it is necessary. Wing flaps and slats are the common movable high-lift devices. Leading-edge slots, leading edge root extensions, and boundary layer control systems are some of the fixed devices. Out of these high lift devices, flaps are of our interest. Flaps are a type of high-lift device used to decrease the stalling speed of an aircraft wing at a given weight.

- Flaps increase lift and thereby reducing stalling speed, and it enables take-off at lower air speed.
- Shorter ground run, reduction in rate of climb due to increase in drag.
- Lower take-off and landing speeds.
- Less wear and tear on brakes.

2.1. LITERATURE SURVEY

From FS Baig AZ, Cheema TA, Aslam Z, Khan YM, Sajid Dar H and Khaliq SB's[1], A New Methodology for Aerodynamic Design and Analysis of a Small Scale Blended Wing Body, 2018, the task of airfoil selection was made easier and more intuitive – a high lift airfoil was the criteria of the center body and a positive moment airfoil was the criteria of the outer wing.

From Martin Masareel's [2], lmprovement of aerodynamic behavior of BWB UAV numerical and experimental investigations, 2016, Lift to drag ratio was represented as a function of the sweep angle of the wing. Changing the sweep angle will have an impact on stability. The interval of 15° to 35° is validated.

From Sanjiv Paudel, Shailendra Rana, Saugat Ghimire, Kshitiz Kumar Subedi, Sudip Bhattrai's [3] Aerodynamic and Stability Analysis of Blended Wing Body Aircraft, 2016, the stability investigation of the BWB shows that the aircraft is statically stable with a positive static margin of 18%. Our design was inspired from this paper.

2.2. MOTIVATION FOR THE RESEARCH WORK

Due to the advancements in current technology of UAV design and its large scope of application in various fields under various environments, it is important to improve the performance of such UAV's through innovative ideas for satisfying future requirements. Thus, undertaking a work on UAV design and performance and application of BWB concept gave a great motivation for us to probe further in UAV technology. As per the recent ASME reports drones are becoming promising Industrial growth potential in near future. Increasing environmental concerns and fuel prices motivate the study of alternative, un-conventional aircraft configurations. One such example is the blended-wing-body configuration, which has been shown to have several advantages over the conventional tube-and-wing aircraft configuration.

3. OBJECTIVES AND PROBLEM STATEMENT

3.1. Problem Description

To design and analyze a typical BWB UAV configuration with and without flaps for low Reynolds number and low speed conditions.

3.2. Objectives

To perform CFD Analysis of BWB UAV with flaps and without flaps and compare their aerodynamic coefficients.

- ✓ To select an appropriate airfoil that satisfies our design requirements by analyzing the selected airfoils suitable for BWB UAV design on XFLR.
- ✓ To design models of Blended Wing Body UAV configuration with and without flaps using Solidworks 2018.
- ✓ To analyze both the designed models of BWB UAV by using ANSYS 18.1.
- ✓ To validate that the proposed BWB UAV with flaps concept offers better aerodynamic characteristics as compared to BWB UAV without flaps.

4. AIRFOIL ANALYSIS AND SELECTION

4.1. Selection of airfoil for the root chord

The majority of the lift is produced by the center body in case of BWB UAV. Therefore it was necessary to choose a high lift airfoil at the root chord. Four high-lift airfoils suitable for blended wing body were chosen and they were analyzed on XFLR and the necessary graphs were plotted. The airfoils that were chosen include S1223, E422, E423, FX74.
Lift and drag coefficients were the main criteria used in order to select the airfoil for the root chord. S1223 was thus selected as it had a high lift coefficient as well as a low drag coefficient value, when compared to the other 3 airfoils.

4.1.1. LIFT COEFFICIENT (C_l) vs. ANGLE OF ATTACK (AOA)

When the airfoil S1223 is compared with the other three airfoils, it shows linear increase in the lift and also has high lift co-efficient at low angle of attack i.e. at 9.75 degrees showing better performance as shown in Fig 4.1.

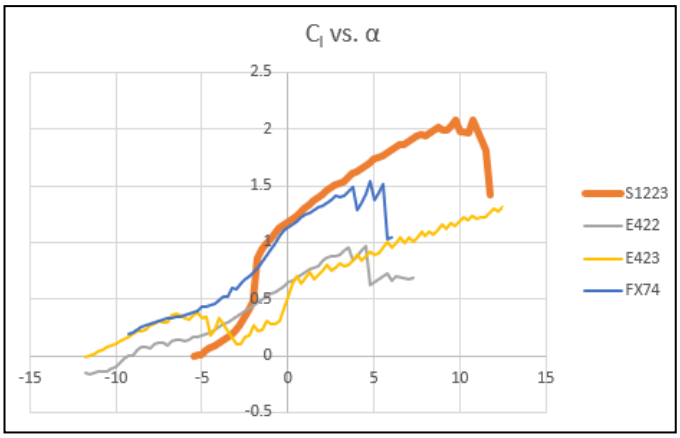

Fig 4.1. C_l vs. α

4.1.2. DRAG COEFFICIENT (C_d) vs. ANGLE OF ATTACK (AOA)

From the Fig 4.2, the obtained drag coefficient for S1223 airfoil is lesser than other three airfoils and its found to be equal to 0.021.

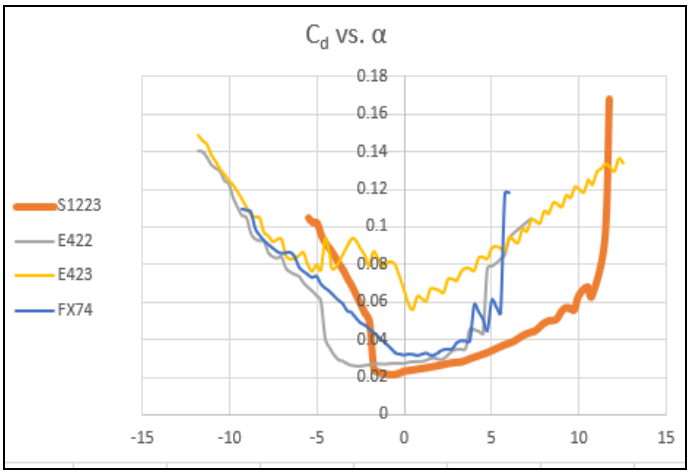

Fig 4.2. C_d vs. α

4.1.3. LIFT COEFFICIENT vs. DRAG COEFFICIENT (C_l vs. C_d)

From the Fig 4.3, it's clear that S1223 airfoil exhibits highest L/D ratio compared to other three airfoils.

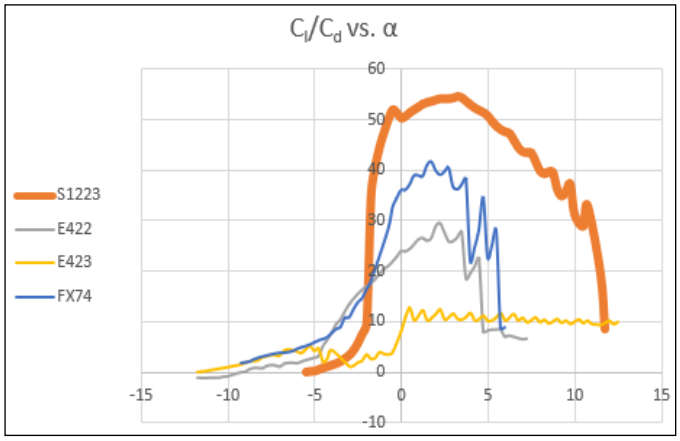

Fig 4.3. C_l vs. C_d

Therefore, S1223 was chosen for the root chord due to its better characteristics amongst the four.

4.2. Selection of airfoil for the tip chord

MH45 has low moment coefficient of $C_{Mc/4}$=0.0145[2]. This was important because for the chosen configuration required the airfoils to produce minimal negative C_M values to make it possible to obtain a positive C_M for the entire wing. This airfoil produces a relatively high C_{LMAX} of 1.28 at Reynolds number 100000. When it is used at the tip of the wing, it provides aerodynamic twist. Therefore, MH45 is chosen at the tip chord.

Characteristics of selected airfoils is summarized in the below Table 4.1

Table 4.1. Characteristics of selected airfoils

PARAMETERS/AIRFOILS	S1223	MH45
$(t/c)_{max}$	12.1%	9.8%
X/C at $(t/c)_{max}$	19.8%	30.0%
Max. Camber	8.1%	1.7%
Position of Max. Camber	49.0%	36.6%
$C_{m,c/4}$	-0.29	0.0145
C_{lmax}	2.2	1.1709
α at C_{lmax}	9.75°	11.25°
$(C_l/C_d)_{max}$	54.48	44.6
C_{dmin}	0.021	0.01327
Placement	Root chord	Tip chord

5. DESIGN OF BWB UAV

Based on the defined objective of the project, we have focused on the geometrical aspects of BWB aircraft. Through literature survey we have selected the BWB UAV design configuration from Sanjiv Paudel, Shailendra Rana, Saugat Ghimire, Kshitiz Kumar Subedi, Sudip Bhattrai, "Aerodynamic and Stability Analysis of Blended Wing Body Aircraft", 2016.

Using MH45 as the tip chord and S1223 as the root chord we have designed BWB UAV with flaps and without flaps whose specifications are given in Table 5.1. The design of BWB UAV without flaps is as shown in Fig 5.1.

Table 5.1. Specifications of Designed BWB UAV

SPECIFICATIONS	
Wing Span (m)	0.36
Root Chord(m)	0.152
Tip Chord(m)	0.02
Taper Ratio	0.13
Sweep angle	33°
Wing twist	-3°
Dihedral angle	0°

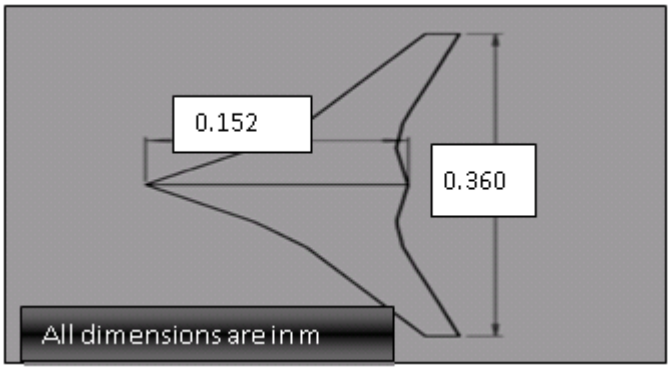

Fig 5.1. Dimensions of BWB UAV without flaps

Dimensions of the flap are as shown in Table 5.2 and the BWB UAV with flaps with specifications are as shown in Fig 5.2.

Table 5.2. Flap dimensions

Root chord of flap (m)	Tip chord of flap (m)	Span (m)	Deflection Angle (°)
0.0214	0.014	0.026	-20°

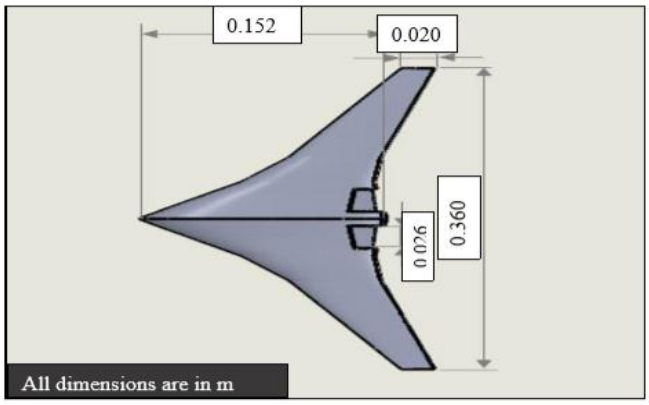

Fig 5.2. Dimensions of BWB UAV with flaps

6. ANALYSIS OF BWB UAV

6.1. GEOMETRY

IGS file exported from Solidworks is imported into geometry of ANSYS FLUENT and the enclosure is created of size 1.5m x 1.5m x 1.5m. The enclosure is as shown in Fig 6.1.

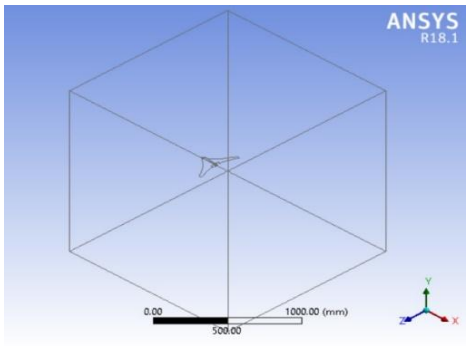

Fig 6.1. Enclosure

6.2. MESHING

Meshing for both the models are done using edge sizing and face meshing operations. The number of elements and the corresponding number of nodes are selected based on grid independence study. Both the models contain tetrahedral elements.

6.2.1 GRID INDEPENDENT STUDY

Grid independence study is important in FLUENT for a certain geometry to get accurate answers. A CFD solution can never be trusted unless we check whether the results depend on the grid or not. The output of the coarser mesh and finer mesh can neither be the same. Therefore, we need to vary the mesh to get the accepted level of tolerance which could be found out from grid independent test. When varying the mesh doesn't affect the result much we can stop and select that minimum mesh size for our final solution output.

- ✓ Grid independent study was done for both the designed models at 20m/s velocity and at 0° angle of attack.
- ✓ In the meshing, number of divisions in the edge sizing operation was chosen as the parameter to be varied.
- ✓ Also, number of elements and nodes from meshing, and lift values from solution were parameterized.
- ✓ Number of divisions in edge sizing operation was varied from 20 to 80 divisions in steps of 5.
- ✓ Number of elements and nodes, lift values were obtained for the respective variation.
- ✓ Values of lift force was plotted against number of elements for both the designs as shown in Fig 6.2 and Fig 6.3.
- ✓ Result variation are not significant after the marked cell size; hence this can be considered as the better mesh for the calculation.

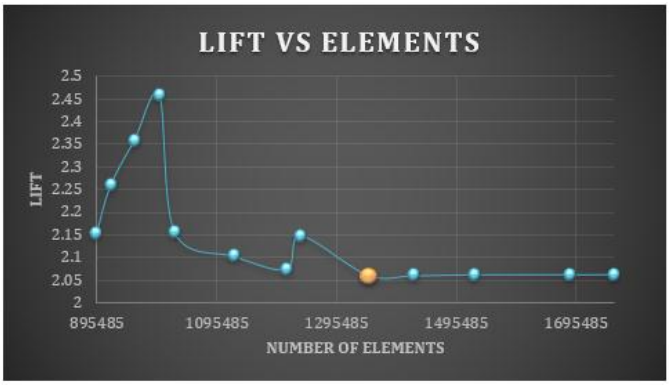

Fig 6.2. Lift vs. Number of elements for without flaps

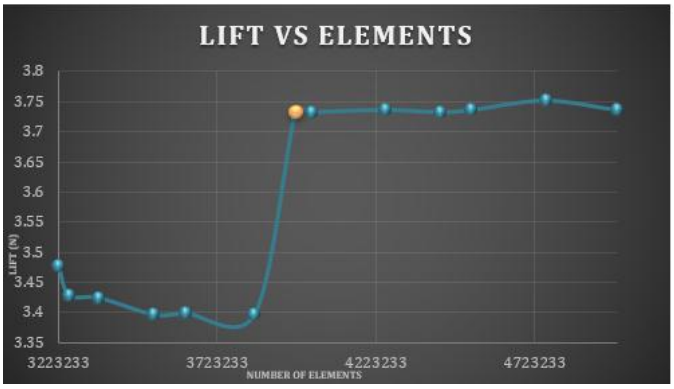

Fig 6.3. Lift vs. Number of elements for with flaps

Therefore, the number of elements and the corresponding number of nodes chosen after grid independent study are as displayed in Table 6.1.

Table 6.1. Node and Element details of BWB UAV

	WITHOUT FLAPS	WITH FLAPS
NODES	249645	725875
ELEMENTS	1348002	3970060

The meshing for both the designs are shown in Fig 6.4 and Fig 6.5.

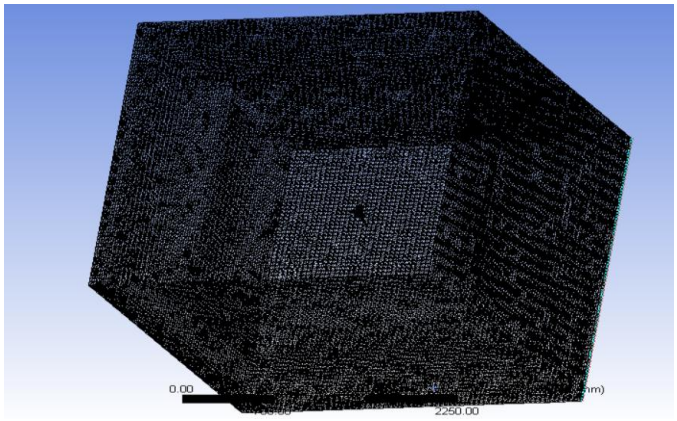

Fig 6.4. Meshing over BWB UAV without flaps

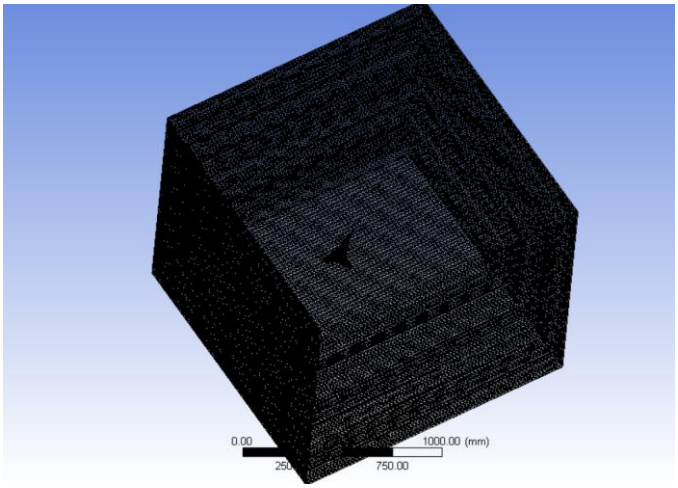

Fig 6.5. Meshing over BWB UAV with flaps

Solver details and boundary conditions are as shown in the Table 6.2 and 6.3 respectively.

Table 6.2. Solver Details

SOLVER DETAILS	
SOLVER	PRESSURE BASED
TIME	STEADY
MODEL	SPALART ALLMARAS
MATERIAL (FLUID)	AIR
SOLUTION INITIALIZATION	STANDARD

Table 6.3. Boundary Conditions

ZONE	TYPE
INLET	VELOCITY
OUTLET	PRESSURE
WALLS	WALL
WING	WALL

7. RESULTS AND DISCUSSIONS

Analysis of the two designs (with and without flaps) were done at five different velocities (10, 15, 20, 25, 30 m/s) and at 5 different angles of attack (-5°, 0°, 5°, 10°, 15°).

7.1. NUMERICAL RESULTS OF BWB UAV WITHOUT FLAPS

The contour of pressure magnitude obtained for various velocities for without flaps deign at 5° AOA are as shown in the Figures 7.1 to 7.5.

The flow accelerates on the upper side of the airfoil and velocity of flow reduces along the lower side, according to Bernoulli's principle the upper surface experiences low pressure and lower surface experiences higher pressure. As the pressure on lower surface is greater than that of incoming flow stream, aircraft is effectively pushed upward normal to the incoming flow stream. At -5° angle of attack, there is very low pressure on the surfaces of the aircraft.

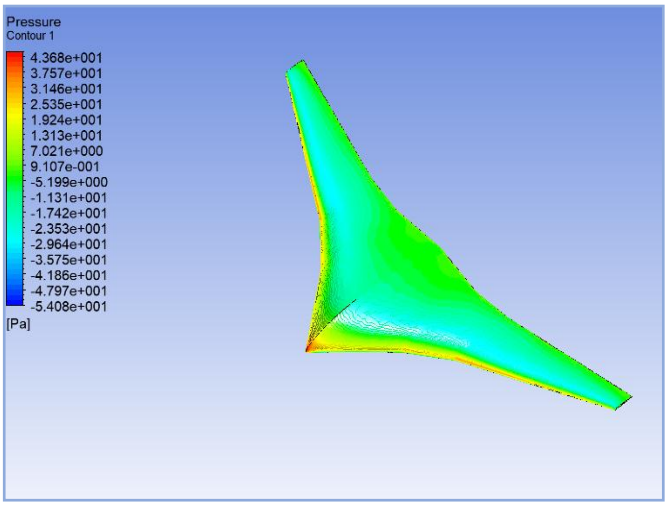

Fig 7.1. Pressure contour at 5° AOA at 10m/s velocity

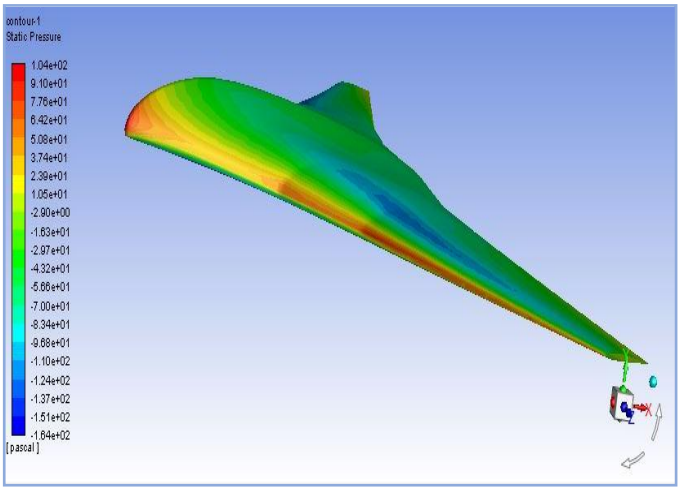

Fig 7.2. Pressure contour at 5° AOA at 15m/s velocity

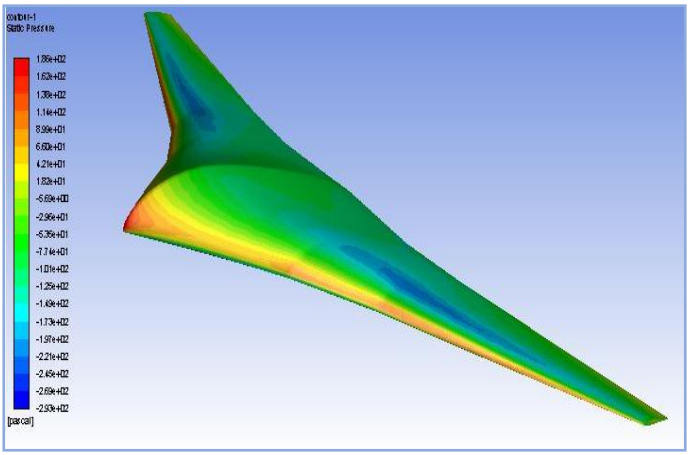

Fig 7.3. Pressure contour at 5° AOA at 20m/s velocity

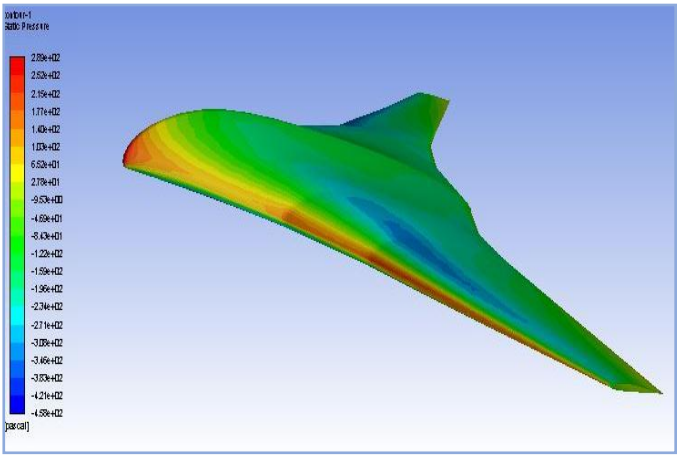

Fig 7.4. Pressure contour at 5° AOA at 25m/s velocity

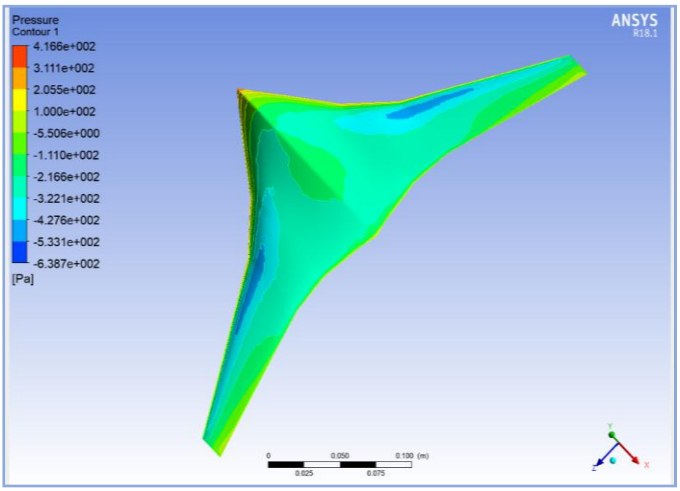

Fig 7.5. Pressure contour at 5° AOA at 30 m/s velocity

At 5° angle of attack at all velocities, the pressure is higher at the leading edge and the bottom surface of the aircraft as shown in the Fig 7.1 to 7.5. The maximum pressure obtained are 43.68 Pa, 104 Pa, 186 Pa, 289 Pa and 416.6 Pa respectively.

7.2. NUMERICAL RESULTS OF BWB UAV WITH FLAPS

The contour of pressure magnitude obtained for various velocities at different angles of attack from CFD simulations are shown in Figures 7.6 to 7.10 for with flaps design. It is seen that flaps design has a higher pressure difference between the lower and upper surface, when compared to without flaps design. Hence, there is more lift generated when flaps are used. Also, as the angle of attack increases, the pressure difference also increases just like the previous design.

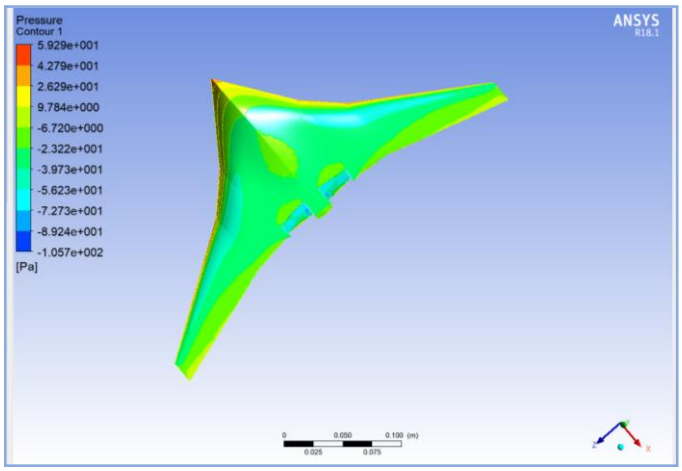

Fig 7.6. Pressure contour at 5° AOA at 10 m/s velocity

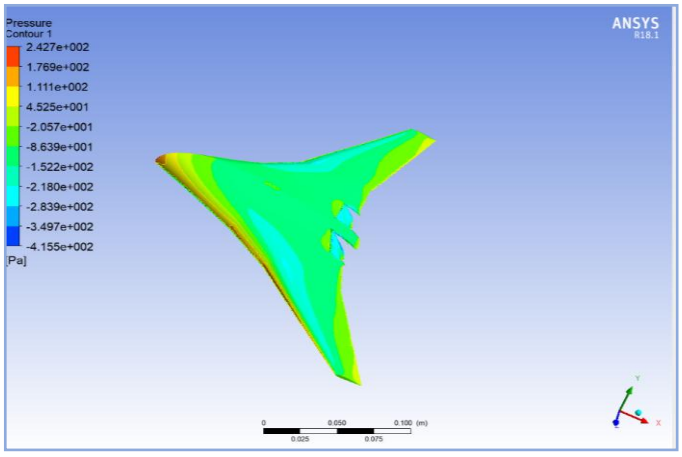

Fig 7.7. Pressure contour at 5° AOA at 15 m/s velocity

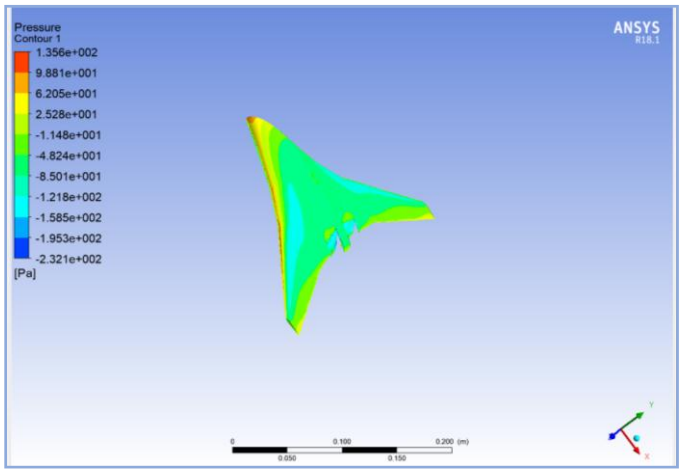

Fig 7.8. Pressure contour at 5° AOA at 20 m/s velocity

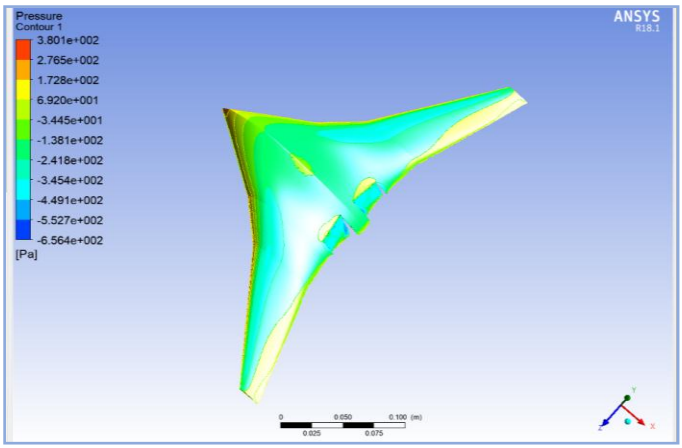

Fig 7.9. Pressure contour at 5° AOA at 25 m/s velocity

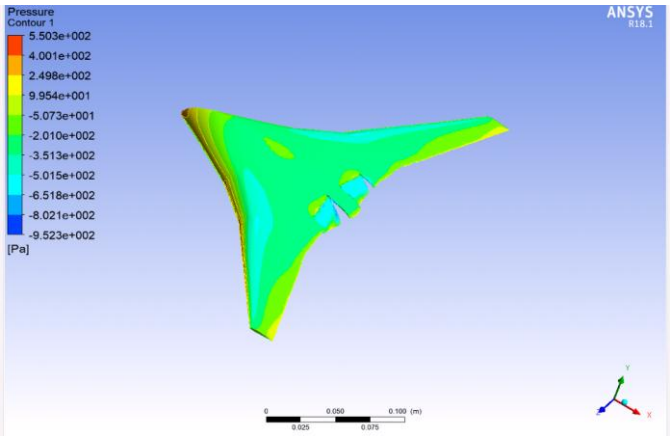

Fig 7.10. Pressure contour at 5° AOA at 30 m/s velocity

At 5° angle of attack at all velocities, the pressure is higher at the leading edge and the bottom surface of the aircraft as shown in the Fig 7.6 to 7.10. The maximum pressure obtained are 59.29 Pa, 135.6 Pa, 242.7 Pa, 380.1 Pa and 550.3 Pa respectively.

7.3. CALCULATIONS AND RESULTS

The lift and drag values are obtained through analysis and the corresponding coefficients of lift and drag are calculated and plotted against angle of attack.

In blended wing body the wings along with fuselage will act as an aerodynamic entity unlike conventional wings.

Surface Area S = 0.0248 m^2;

Density of Air ρ = 1.225 Kg/m^3;

Velocity v = 10 m/s;

Using their respective formulas, coefficient of lift and coefficient of drag are calculated.

At -5°Angle of attack and 10 m/s velocity for BWB UAV **without flaps,**

L = -0.2739 N; D = 0.0372 N;

$$C_L = \frac{2L}{\rho * v^2 * S} = \frac{2*(-0.2739)}{1.225*10^2*0.0248} = -0.1803$$

$$C_D = \frac{2D}{\rho * v^2 * S} = \frac{2*0.0372}{1.225*10^2*0.0248} = 0.0245$$

The Table 7.1 summarizes the lift and drag coefficients calculated for without flaps design, for all angles of attack at 10 m/s velocity.

WITHOUT FLAPS (v = 10 m/s)					
AOA	Lift	C_L	Drag	C_D	C_L/C_D
-5°	-0.2739	-0.1803	0.0372	0.0245	-7.3592
0°	0.3585	0.236	0.0279	0.0184	12.8261
5°	0.5084	0.3347	0.0377	0.0248	13.496
10°	0.7071	0.4655	0.048	0.0316	14.731
15°	0.7805	0.5138	0.0507	0.0334	15.3832

Table 7.1. C_L and C_D values at different angle of attack at 10 m/s (without flaps)

At -5° Angle of attack and 10 m/s velocity for BWB UAV **with flaps**,

L = -0.237 N; D = 0.0396 N;

$$C_L = \frac{2L}{\rho * v^2 * S} = \frac{2*(-0.237)}{1.225*10^2*0.0248} = -0.156$$

$$C_D = \frac{2D}{\rho * v^2 * S} = \frac{2*0.0396}{1.225*10^2*0.0248} = 0.0261$$

The Table 7.2 summarizes the lift and drag coefficients calculated for with flaps design, for all angles of attack at 10 m/s velocity.

Table 7.2. C_L and C_D values at different angle of attack at 10 m/s (with flaps)

WITH FLAPS (v = 10 m/s)					
AOA	Lift	C_L	Drag	C_D	C_L/C_D
-5°	-0.237	-0.156	0.0396	0.0261	-5.977
0°	0.4908	0.3231	0.0357	0.0235	13.7489
5°	0.7431	0.4892	0.0472	0.0311	15.7299
10°	0.8629	0.5681	0.051	0.0336	16.9077
15°	0.9351	0.6156	0.0533	0.0351	17.5385

The Fig 7.11 and Fig 7.12 shows the comparison of lift and drag coefficients of both the designs (with and without flaps). It is seen that C_L and C_D is more for the with flaps design. The maximum value of C_L obtained is 0.6156 and the corresponding C_D value is 0.0351 for with flaps design, while the maximum C_L and C_D values for without flaps design are 0.5138 and 0.0344 respectively.

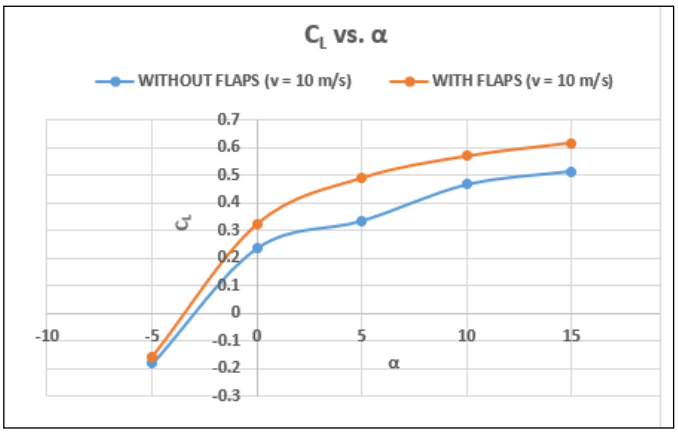

Fig 7.11. C_L vs. α at 10 m/s velocity

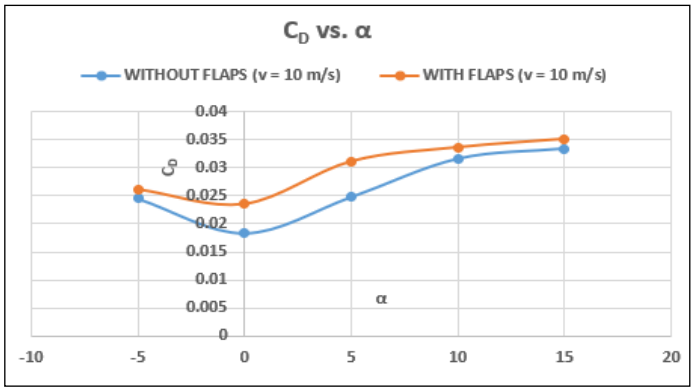

Fig 7.12. C_D vs. α at 10 m/s velocity

Further drag polar was drawn at 10m/s velocity. Drag polar is a curve which expresses the relation between the lift and drag of an aircraft, conveyed in terms of the reliance of the drag coefficient on the lift coefficient. Fig 7.13 will interpret the drag polar at 10m/s velocity. Also, the Fig 7.14 shows the plot of C_L/C_D and angle of attack (α). The maximum C_L/C_D ratio obtained is 15.38 for without flaps BWB UAV and 17.5385 for with flaps BWB UAV, both at 15° angle of attack.

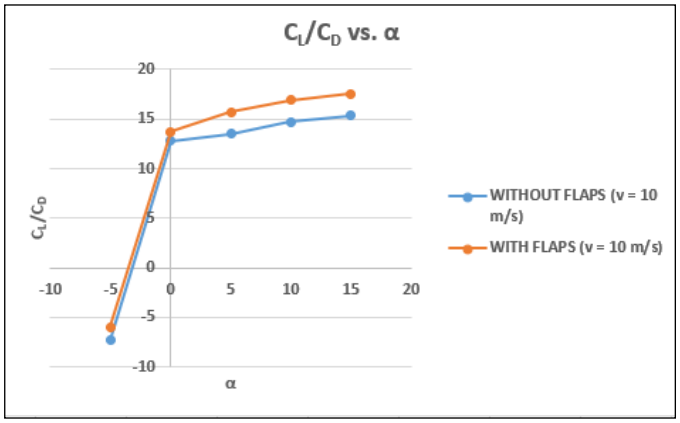

Fig 7.13. C_L vs. C_D at 10 m/s velocity

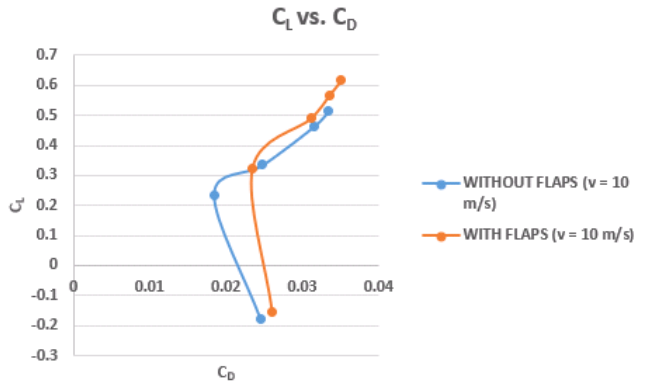

Fig 7.14. C_L/C_D vs. α at 10 m/s velocity

At 15 m/s Velocity

The calculated coefficients of lift and drag values at 15 m/s velocity for without flaps and with flaps are as shown in the Table 7.3 and Table 7.4 respectively. The Fig 7.15 and Fig 7.16 shows the comparison of both the designs. Also Fig 7.17 and Fig 7.18 represents drag polar and C_L/C_D vs. angle of attack (α) respectively.

Table 7.3. C_L and C_D values at different angles of attack at 15m/s (without flaps)

WITHOUT FLAPS (v = 15 m/s)					
AOA	Lift	C_L	Drag	C_D	C_L/C_D
-5°	-0.7905	-0.2313	0.0824	0.0241	-9.5975
0°	0.9833	0.2877	0.0687	0.0201	14.3134
5°	1.2789	0.3742	0.0875	0.0256	14.6172
10°	1.8596	0.5441	0.1142	0.0334	16.2904
15°	2.1508	0.6293	0.1271	0.0372	16.9167

Table 7.4. C_L and C_D values at different angles of attack at 15m/s (with flaps)

WITH FLAPS (v = 15 m/s)					
AOA	Lift	C_L	Drag	C_D	C_L/C_D
-5°	-0.7563	-0.2213	0.0875	0.0256	-8.6445
0°	1.2034	0.3521	0.0793	0.0232	15.1767
5°	1.7984	0.5262	0.1066	0.0312	16.8654
10°	2.1241	0.6215	0.1237	0.0362	17.1685
15°	2.429	0.7107	0.1309	0.0383	18.5561

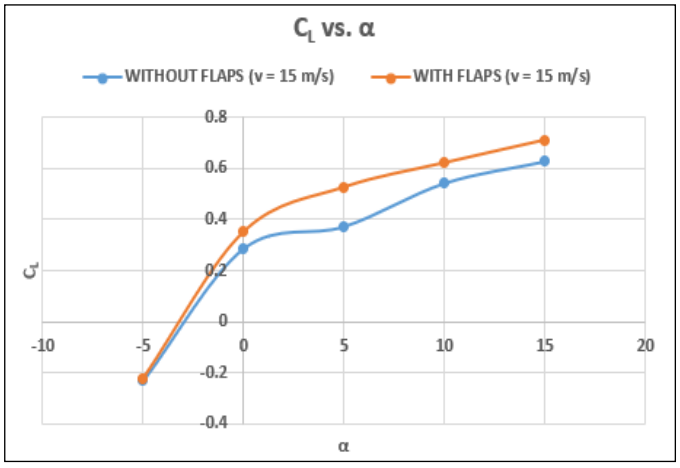

Fig 7.15. C_L vs. α at 15 m/s velocity

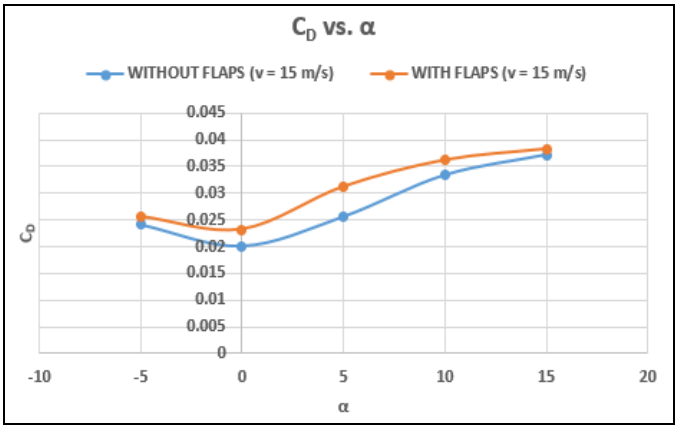

Fig 7.16. C_D vs. α at 15 m/s velocity

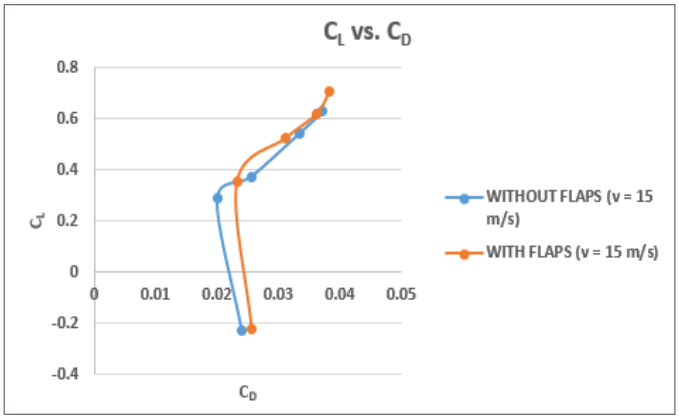

Fig 7.17. C_L vs. C_D at 15 m/s velocity

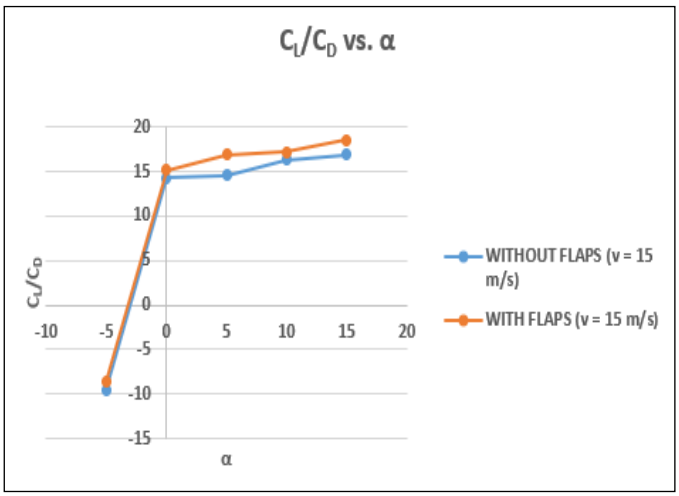

Fig 7.18. C_L/C_D vs. α at 15 m/s velocity

At 20 m/s Velocity

The calculated coefficients of lift and drag values at 20 m/s velocity for without flaps and with flaps are as shown in the Table 7.5 and Table 7.6 respectively. The Figures 7.19 and 7.20 shows the comparison of both the designs. Also Fig 7.21 and Fig 7.22 represents drag polar and C_L/C_D vs. angle of attack (α) respectively.

Table 7.5. C_L and C_D values at different angles of attack at 20 m/s (without flaps)

WITHOUT FLAPS (v = 20 m/s)					
AOA	Lift	C_L	Drag	C_D	C_L/C_D
-5	-2.0999	-0.3456	0.1896	0.0312	11.0769
0	2.061	0.3392	0.1404	0.0231	14.684
5	2.798	0.4605	0.1689	0.0278	16.5647
10	3.9695	0.6533	0.2218	0.0365	17.8986
15	4.3936	0.7231	0.2436	0.0401	18.0324

Table 7.6. C_L and C_D values at different angles of attack at 20m/s (with flaps)

WITH FLAPS (v = 20 m/s)					
AOA	Lift	C_L	Drag	C_D	C_L/C_D
-5	-1.8975	-0.3123	0.2218	0.0365	-8.5562
0	3.7319	0.6142	0.195	0.0321	19.134
5	4.207	0.6924	0.2151	0.0354	19.5593
10	4.7648	0.7842	0.2376	0.0391	20.0563
15	5.4265	0.8931	0.2546	0.0419	21.315

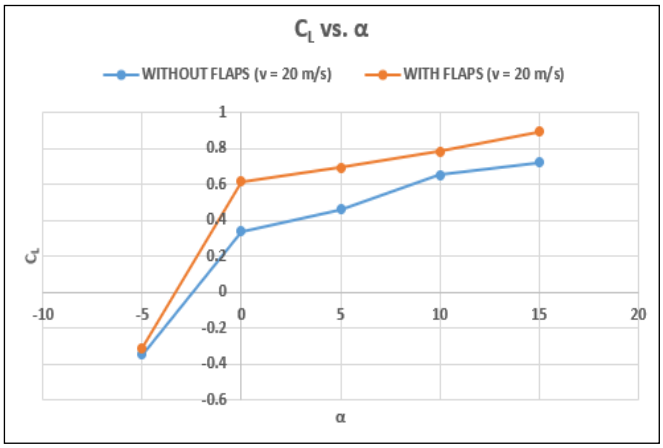

Fig 7.19. C_L vs. α at 20 m/s velocity

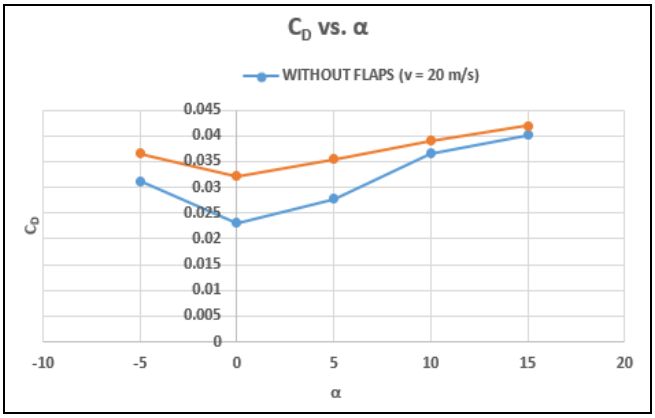

Fig 7.20. C_D vs. α at 20 m/s velocity

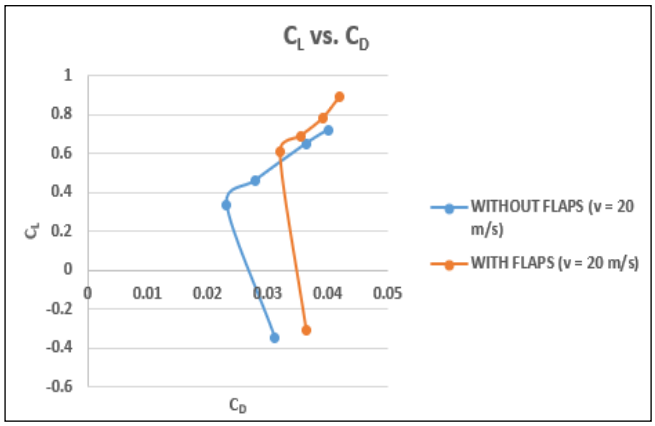

Fig 7.21. C_L vs. C_D at 20 m/s velocity

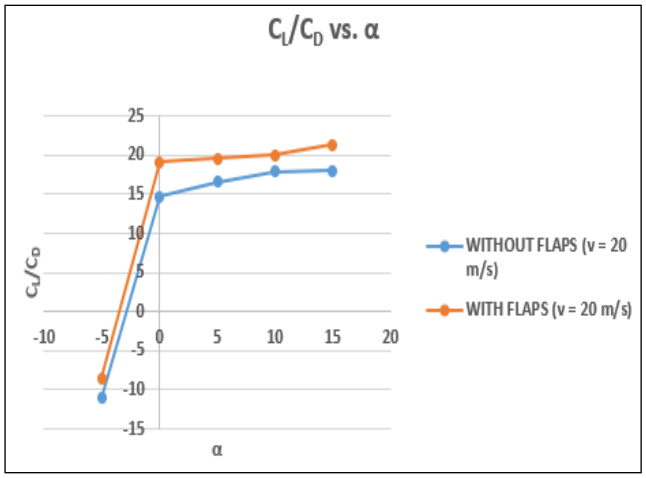

Fig 7.22. C_L/C_D vs. α at 20 m/s velocity

At 25 m/s Velocity

The calculated coefficients of lift and drag values at 25 m/s velocity for without flaps and with flaps are as shown in the Table 7.7 and Table 7.8 respectively. The Figures 7.23 and 7.24 shows the comparison of both the designs. Also Figures 7.25 and 7.26 represents drag polar and C_L/C_D vs. angle of attack (α) respectively.

Table 7.7. C_L and C_D values at different angles of attack at 25 m/s (without flaps)

WITHOUT FLAPS (v = 25 m/s)					
AOA	Lift	C_L	Drag	C_D	C_L/C_D
-5°	-4.5798	-0.4824	0.3047	0.0321	-15.028
0°	3.5298	0.3718	0.2411	0.0254	14.6378
5°	4.951	0.5215	0.2858	0.0301	17.3256
10°	6.8194	0.7183	0.3674	0.0387	18.5607
15°	7.8191	0.8236	0.3997	0.0421	19.5629

Table 7.8. C_L and C_D values at different angles of attack at 25 m/s (with flaps)

WITH FLAPS (v = 25 m/s)					
AOA	Lift	C_L	Drag	C_D	C_L/C_D
-5°	-3.9522	-0.4163	0.3332	0.0351	-11.8604
0°	6.2203	0.6552	0.3047	0.0321	20.4112
5°	7.9187	0.8341	0.3693	0.0389	21.4422
10°	9.057	0.954	0.394	0.0415	22.9880
15°	9.7985	1.0321	0.4082	0.043	24.0023

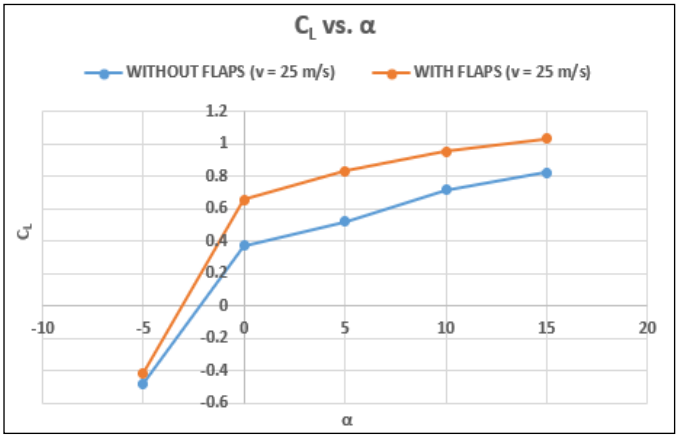

Fig 7.23. C_L vs. α at 25 m/s velocity

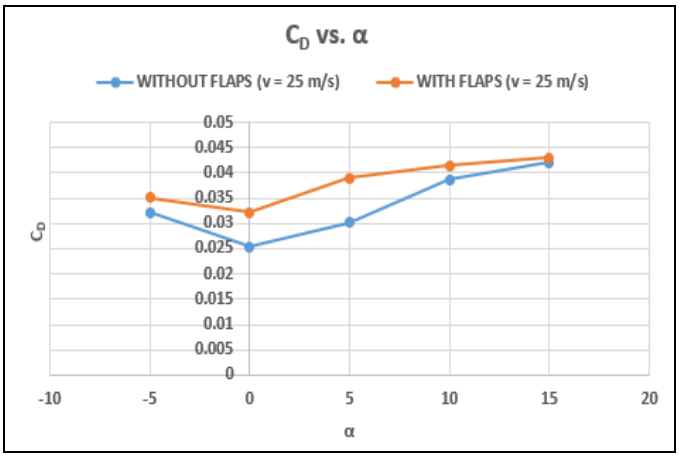

Fig 7.24. C_D vs. α at 25 m/s velocity

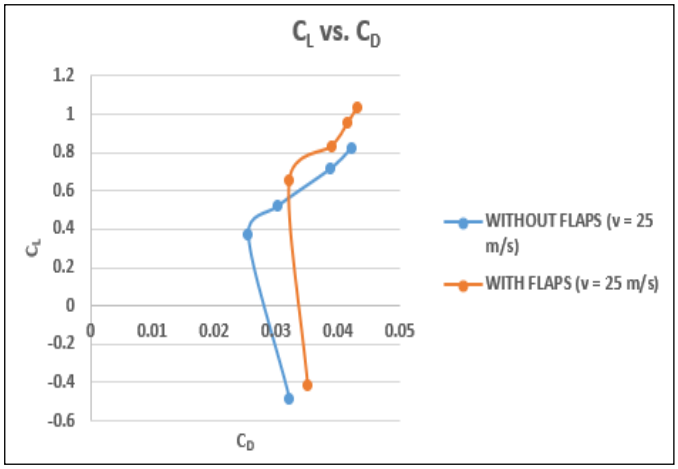

Fig 7.25. C_L vs. C_D at 25 m/s velocity

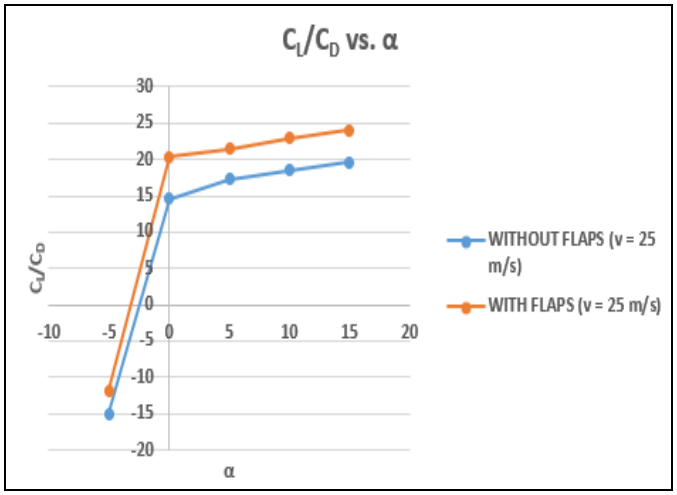

Fig 7.26. C_L/C_D vs. α at 25 m/s velocity

At 30 m/s Velocity

The calculated coefficients of lift and drag values at 30 m/s velocity for without flaps and with flaps are as shown in the Table 7.9 and Table 7.10 respectively. The Fig 7.27 and Fig 7.28 shows the comparison of both the designs. Also Fig 7.29 and Fig 7.30 represents drag polar and C_L/C_D vs. angle of attack (α) respectively.

Table 7.9 . C_L and C_D values at different angles of attack at 30 m/s (without flaps)

WITHOUT FLAPS (v = 30 m/s)					
AOA	**Lift**	**C_L**	**Drag**	**C_D**	**C_L/C_D**
-5°	-10.7509	-0.7864	0.4949	0.0362	-21.7238
0°	6.9913	0.5114	0.4074	0.0298	17.1611
5°	11.5274	0.8432	0.5482	0.0401	21.0274
10°	13.3388	0.9757	0.6234	0.0456	21.3969
15°	15.518	1.1351	0.7123	0.0521	21.7869

Table 7.10. C_L and C_D values at different angles of attack at 30 m/s (with flaps)

WITH FLAPS (v = 30 m/s)					
AOA	**Lift**	**C_L**	**Drag**	**C_D**	**C_L/C_D**
-5°	-7.7419	-0.5663	0.5961	0.0436	-12.9885
0°	9.8664	0.7217	0.5427	0.0397	18.1788
5°	12.6347	0.9242	0.6166	0.0451	20.4922
10°	16.453	1.2035	0.6808	0.0498	24.1667
15°	18.4039	1.3462	0.7273	0.0532	25.3045

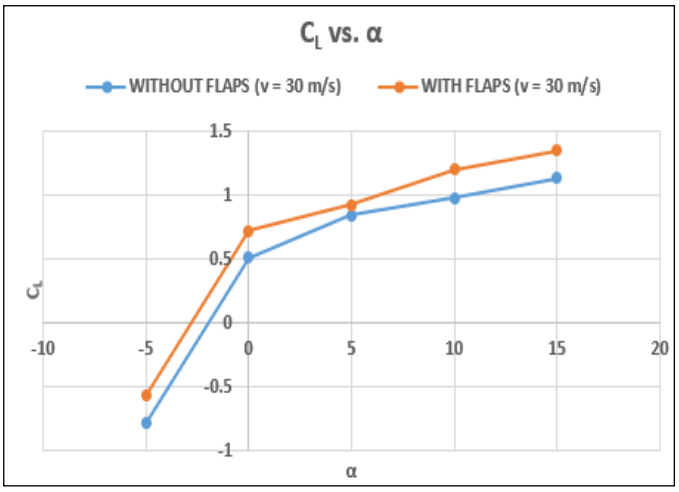

Fig 7.27. C_L vs. α at 30 m/s velocity

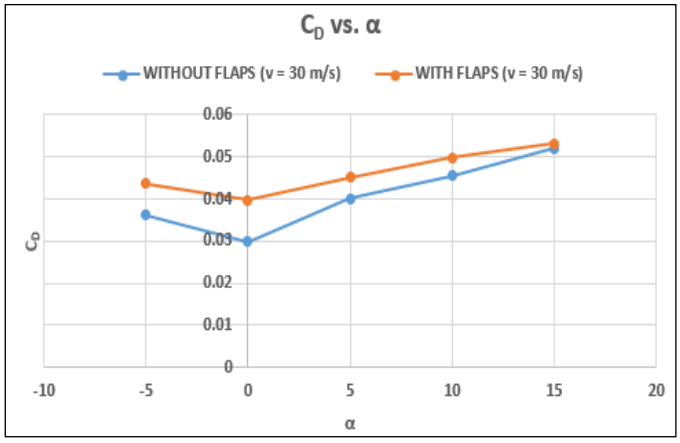

Fig 7.28. C_D vs. α at 30 m/s velocity

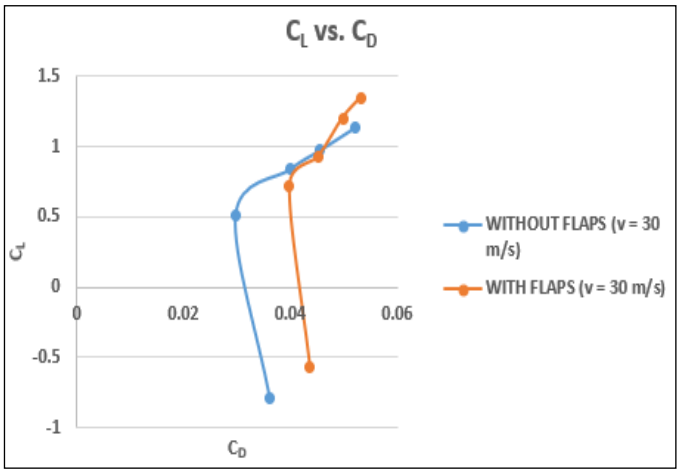

Fig 7.29. C_L vs. C_D at 30 m/s velocity

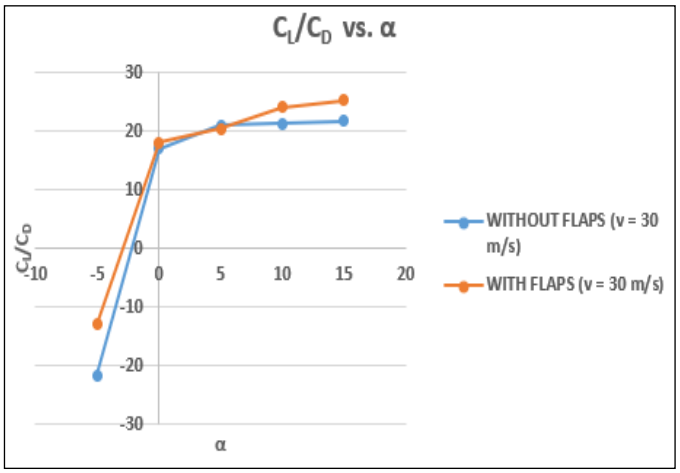

Fig 7.30. C_L/C_D vs. α at 30 m/s velocity

7.3. COMPARISON OF THE RESULTS

The lift to drag ratio (L/D) is the amount of lift generated by the wing compared to its drag. It is always best to have a greater L/D ratio. The lift producing devices such as flaps affect the production of lift which will vary with changes in angle of attack. Based on the analysis, it is seen that there is an increase in L/D ratio when flaps are added to the design, at all velocities. The Table 7.11 shows the percentage increase in L/D ratio at 15° angle of attack of the BWB UAV with flaps compared to the BWB UAV without flaps design at different velocities. The Fig 7.31 interprets the plot of L/D vs. Velocity for both the designs at 15° angle of attack.

Table 7.11. Comparison of L/D ratios of the two designs at 15° AOA

Velocity (m/s)	$(L/D)_{without\ flaps}$	$(L/D)_{with\ flaps}$	Increase in L/D ratio (%)
10	15.3832	17.5385	14.01
15	16.9167	18.5561	9.69
20	18.0324	21.315	18.2
25	19.5629	24.0023	22.69
30	21.7869	25.345	16.33

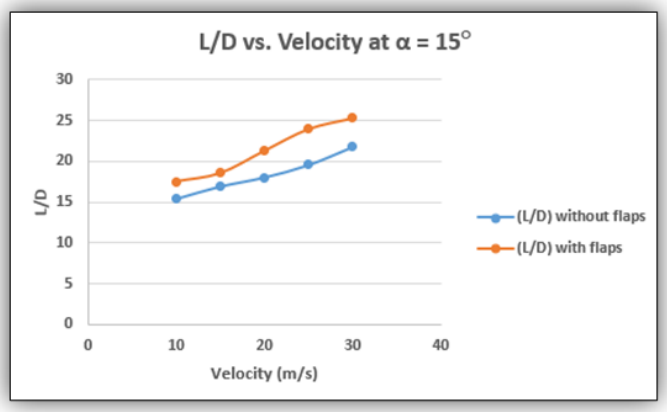

Fig 7.31. L/D vs. Velocity at 15° Angle of attack

8. CONCLUSION AND FUTURE SCOPE

8.1. CONCLUSION

- From the results, L/D ratio obtained for the BWB UAV with flaps offers a maximum value of 25, which is much greater than that of conventional aircraft that have a maximum of around 16.
- Flaps indeed increase the lift produced when compared to the without flaps design.
- This increase in lift is due to the increase in the difference in the pressure values on the lower and upper surfaces of the BWB.
- Also, design with flaps has a greater L/D ratio when compared to without flaps design. A greater or more favorable L/D ratio is typically one of the major goals of aircraft design; since a particular aircraft's required lift

is set by its weight, delivering that lift with lower drag is very desirable.

- Although flaps increase the drag coefficient of an aircraft due to higher induced drag, it can be seen from the results that as the angle of attack increases, at higher angles of attack (15°), the drag values of both the design becomes equal. Simultaneously, lift value of with-flaps design is higher than without-flaps design. Since, drag is almost equal in both the designs, but lift value is more when flaps are used, hence the L/D ratio increases to a much greater values at higher angles of attack (around 22.69% increase at v = 25 m/s).
- It is also seen that from the C_L vs. α plots, stalling of the BWB UAV has not taken place till 15° angle of attack. This is very useful because it implies that the BWB UAV can fly at higher angles of attack without stalling.

8.2. FUTURE SCOPE

- The model can be tested experimentally in the wind tunnel to validate the analytical results.
- Flaps can be analyzed and tested at different deflection angles.
- But using the combination of leading and trailing edge high lift devices, it is possible to reduce the drag. An example could be Co-Flow Jet (CFJ) wing having an upper surface with an injection slot after the leading edge and a suction slot before the trailing edge, to augment lift, increase the stall margin and reduce drag.
- Through our literature survey, we investigated that NASA Supercritical airfoils can be used to develop BWB UAV, which can fly at transonic velocities. Due to time constraints and non-availability of supersonic wind tunnel facility, it wasn't possible for us to develop a supersonic BWB UAV. Future work might include developing a supersonic BWB UAV with the combination of leading and trailing edge high lift devices.
- Performance parameters like stall speed can be calculated for the BWB UAV.

REFERENCES

[1] Baig AZ, Cheema TA , Aslam Z, Khan YM, Sajid Dar H and Khaliq SB, A New Methodology for Aerodynamic Design and Analysis of a Small Scale Blended Wing Body, 2018.

[2] Sanjiv Paudel, Shailendra Rana, Saugat Ghimire, Kshitiz Kumar Subedi, Sudip Bhattrai, Aerodynamic and Stability Analysis of Blended Wing Body Aircraft, 2016.

[3] Martin Masereel, Improvement of the aerodynamic behavior of a blended wing body unmanned aerial vehicle: numerical and experimental investigations, 2016.

[4] Paulinus Peter Chukwuemeka Okonkwo "Conceptual Design Methodology for Blended Wing Body Aircraft", May 19, 2016.

[5] Melvin Philip, Venkatesh Kusnur , Design Optimization Of A Ducted Fan Blended Wing Body UAV Using CFD Analysis ,2015.

[6] R. M. Martínez, "Design and Analysis of the Control and Stability of a Blended Wing Body Aircraft," CEAS 2015, no. May, pp. 1–14, 2014.

[7] Wirachman Wisnoe , Rizal Effendy Mohd Nasir , Wahyu Kuntjoro, and Aman Mohd Ihsan Mamat, Wind Tunnel Experiments and CFD Analysis of Blended Wing Body (BWB) Unmanned Aerial Vehicle (UAV) at Mach 0.1 and Mach 0.3, 2009.

[8] T. Ikeda and C. Bil, "Aerodynamic Analysis of a Blended-Wing-Body Aircraft Configuration," SICE Annu. Conf. 2005, no. March, pp. 1858–1863, 2005.

[9] Wirachman Wisnoe, Wahyu Kuntjoro, for low subsonic operation, Aerodynamic performance of UiTM BWB-UAV,2002.

[10] R. H. Liebeck, "Design of the Blended Wing Body Subsonic Transport," J. Aircr., vol. 41, no. 1, pp. 10–25, 1988.

LIST OF ABBREVIATIONS

BWB - Blended Wing Body

UAV - Unmanned Aerial Vehicle

AOA - Angle of Attack

ASME - American Society of Mechanical Engineers

CFD - Computational Fluid Dynamics

α - Angle of attack

$C_{Mc/4}$- Coefficient of moment at quarter chord

C_l - Coefficient of lift for an airfoil

C_d - Coefficient of drag for an airfoil

C_L - Coefficient of Lift for BWB UAV

C_D - Coefficient of Drag for BWB UAV

L - Lift force

D - Drag force

S - Surface Area

ρ - Density of Air

v - Velocity